Figure S1

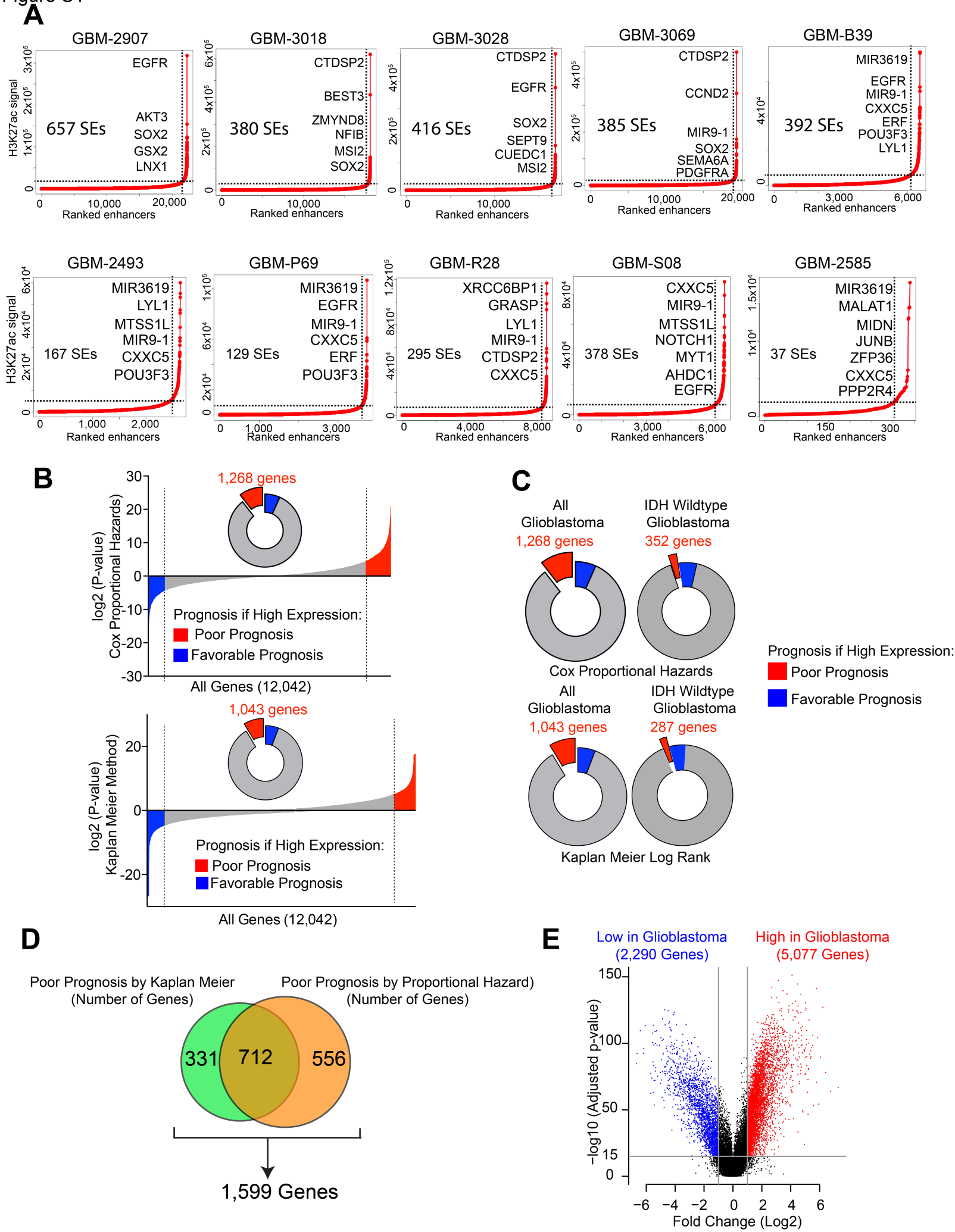
A
GBM-2907
657 SEs
EGFR
AKT3
SOX2
GSX2
LNX1
GBM-3018
380 SEs
CTDSP2
BEST3
ZMYND8
NFIB
MSI2
SOX2
GBM-3028
416 SEs
CTDSP2
EGFR
SOX2
SEPT9
CUEDC1
MSI2
GBM-3069
385 SEs
CTDSP2
CCND2
MIR9-1
SOX2
SEMA6A
PDGFRA
GBM-B39
392 SEs
MIR3619
EGFR
MIR9-1
CXXC5
ERF
POU3F3
LYL1
H3K27ac signal
Ranked enhancers
GBM-2493
167 SEs
MIR3619
LYL1
MTSS1L
MIR9-1
CXXC5
POU3F3
GBM-P69
129 SEs
MIR3619
EGFR
MIR9-1
CXXC5
ERF
POU3F3
GBM-R28
295 SEs
XRCC6BP1
GRASP
LYL1
MIR9-1
CTDSP2
CXXC5
GBM-S08
378 SEs
CXXC5
MIR9-1
MTSS1L
NOTCH1
MYT1
AHDC1
EGFR
GBM-2585
37 SEs
MIR3619
MALAT1
MIDN
JUNB
ZFP36
CXXC5
PPP2R4
B
1,268 genes
log2 (P-value)
Cox Proportional Hazards
Prognosis if High Expression:
Poor Prognosis
Favorable Prognosis
All Genes (12,042)
1,043 genes
log2 (P-value)
Kaplan Meier Method)
Prognosis if High Expression:
Poor Prognosis
Favorable Prognosis
All Genes (12,042)
C
All Glioblastoma
1,268 genes
IDH Wildtype Glioblastoma
352 genes
Cox Proportional Hazards
All Glioblastoma
1,043 genes
IDH Wildtype Glioblastoma
287 genes
Kaplan Meier Log Rank
Prognosis if High Expression:
Poor Prognosis
Favorable Prognosis
D
Poor Prognosis by Kaplan Meier
(Number of Genes)
Poor Prognosis by Proportional Hazard)
(Number of Genes)
331
712
556
1,599 Genes
E
Low in Glioblastoma
(2,290 Genes)
High in Glioblastoma
(5,077 Genes)
−log10 (Adjusted p-value)
Fold Change (Log2)

Figure S1. In silico super-enhancer screen identifies potential glioblastoma stem cell specific therapeutic targets, related to Figure 1.

(A) Super-enhancer hockey-stick plots show all ranked enhancers called from 10 glioblastoma primary tissue samples (GBM-2907, GBM-3018, GBM-3028, GBM-3069, GBM-B39, GBM-2493, GBM-P69, GBM-R28, GBM-S08, GBM-2585). Enhancers were ranked based on the difference between the H3K27ac signal from ChIP-seq data and the respective matched ChIP input file. Super-enhancers were defined by the ROSE algorithm.

(B) All genes present in the glioblastoma TCGA HG-U133A microarray dataset were analyzed for prognostic significance based on mRNA expression levels using (top) the Cox proportional hazards test or (bottom) log rank analysis with patients with greater than the average (mean) expression in the "High expression" group and others in the "Low expression" group.

(C) All genes present in the glioblastoma TCGA HG-U133A microarray dataset were analyzed for prognostic significance based on mRNA expression levels using (top) the Cox proportional hazards test or (bottom) log rank analysis with patients with greater than the average (mean) expression in the "High expression" group and others in the "Low expression" group. Survival analysis was performed across all glioblastoma patients (left) or restricted to IDH wildtype glioblastoma patients (right).

(D) Venn diagram illustrating overlaps between genes with poor prognosis as determined in (B).

(E) Volcano plot showing differentially expressed genes between glioblastoma TCGA RNA-seq data and the GTEx normal brain RNA-seq dataset, as derived from (54). Log2 Fold change > 1, FDR-corrected p-value < 1e-15.

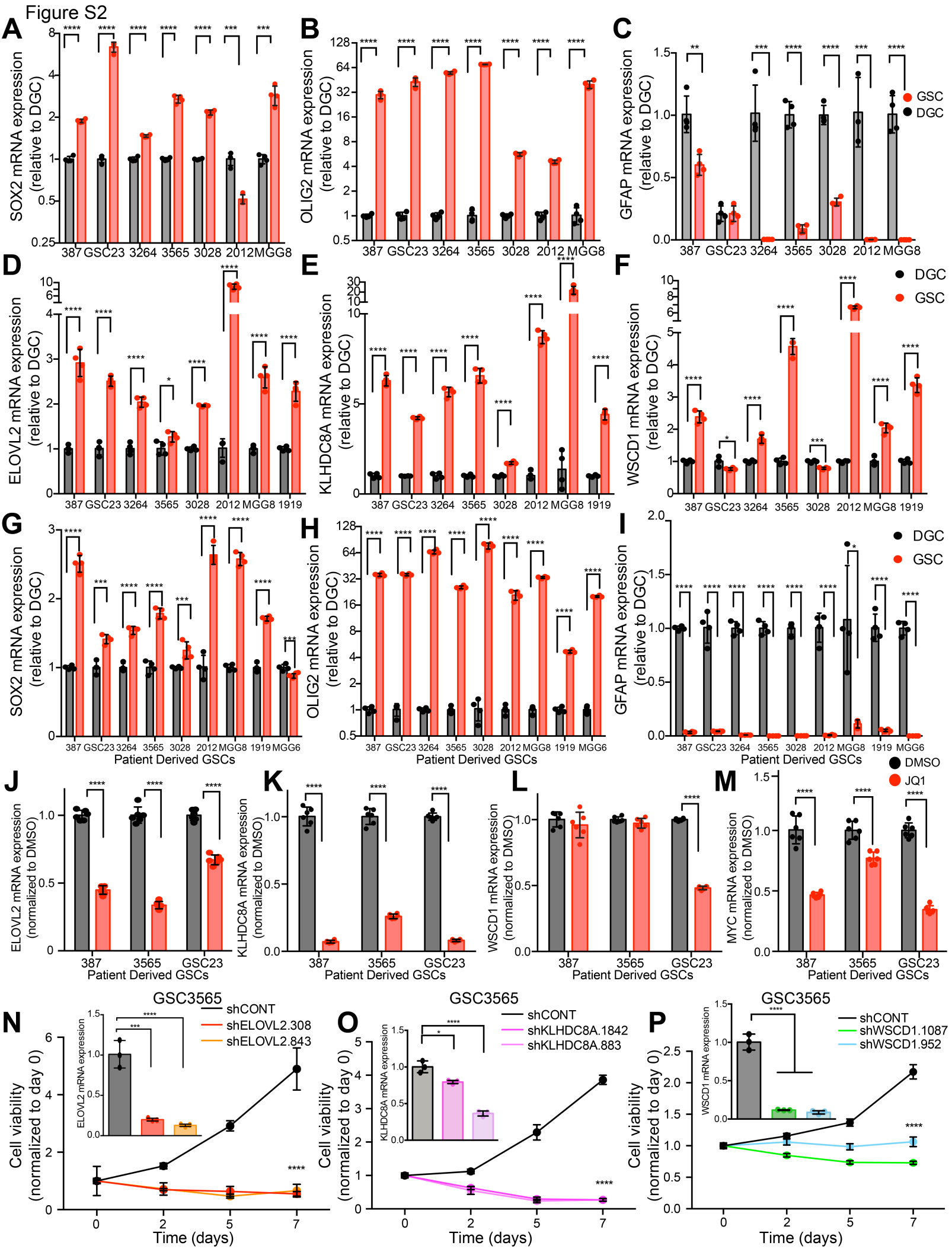
Figure S2
A
SOX2 mRNA expression (relative to DGC)
387 GSC23 3264 3565 3028 2012 MGG8
B
OLIG2 mRNA expression (relative to DGC)
387 GSC23 3264 3565 3028 2012 MGG8
C
GFAP mRNA expression (relative to DGC)
GSC
DGC
387 GSC23 3264 3565 3028 2012 MGG8
D
ELOVL2 mRNA expression (relative to DGC)
387 GSC23 3264 3565 3028 2012 MGG8 1919
E
KLHDC8A mRNA expression (relative to DGC)
387 GSC23 3264 3565 3028 2012 MGG8 1919
F
DGC
GSC
WSCD1 mRNA expression (relative to DGC)
387 GSC23 3264 3565 3028 2012 MGG8 1919
G
SOX2 mRNA expression (relative to DGC)
387 GSC23 3264 3565 3028 2012 MGG8 1919 MGG6
Patient Derived GSCs
H
OLIG2 mRNA expression (relative to DGC)
387 GSC23 3264 3565 3028 2012 MGG8 1919 MGG6
Patient Derived GSCs
I
DGC
GSC
GFAP mRNA expression (relative to DGC)
387 GSC23 3264 3565 3028 2012 MGG8 1919 MGG6
Patient Derived GSCs
J
ELOVL2 mRNA expression (normalized to DMSO)
387 3565 GSC23
Patient Derived GSCs
K
KLHDC8A mRNA expression (normalized to DMSO)
387 3565 GSC23
Patient Derived GSCs
L
WSCD1 mRNA expression (normalized to DMSO)
387 3565 GSC23
Patient Derived GSCs
M
DMSO
JQ1
MYC mRNA expression (normalized to DMSO)
387 3565 GSC23
Patient Derived GSCs
N
GSC3565
shCONT
shELOVL2.308
shELOVL2.843
ELOVL2 mRNA expression
Cell viability (normalized to day 0)
Time (days)
O
GSC3565
shCONT
shKLHDC8A.1842
shKLHDC8A.883
KLHDC8A mRNA expression
Cell viability (normalized to day 0)
Time (days)
P
GSC3565
shCONT
shWSCD1.1087
shWSCD1.952
WSCD1 mRNA expression
Cell viability (normalized to day 0)
Time (days)

Figure S2. Glioblastoma stem cell specific super-enhancer associated genes are essential for glioblastoma stem cell proliferation, related to Figure 2.

(A) qPCR analysis of mRNA expression of SOX2 in 7 matched GSCs and DGCs. Student t-test was used to assess statistical significance with four technical replicates. ***, $p < 0.001$. ****, $p < 0.0001$.

(B) qPCR analysis of mRNA expression of OLIG2 in 7 matched GSCs and DGCs. Student t-test was used to assess statistical significance with four technical replicates. ****, $p < 0.0001$.

(C) qPCR analysis of mRNA expression of GFAP in 7 matched GSCs and DGCs. Student t-test was used to assess statistical significance with four technical replicates. **, $p < 0.01$. ***, $p < 0.001$. ****, $p < 0.0001$.

(D) qPCR analysis of mRNA expression of ELOVL2 in a second derivation of 8 matched GSCs and DGCs. Student t-test was used to assess statistical significance with four technical replicates. * , $p < 0.05$, ***, $p < 0.001$. ****, $p < 0.0001$.

(E) qPCR analysis of mRNA expression of KLHDC8A in a second derivation of 8 matched GSCs and DGCs. Student t-test was used to assess statistical significance with four technical replicates. * , $p < 0.05$, ***, $p < 0.001$. ****, $p < 0.0001$.

(F) qPCR analysis of mRNA expression of WSCD1 in a second derivation of 8 matched GSCs and DGCs. Student t-test was used to assess statistical significance with four technical replicates. * , $p < 0.05$, ***, $p < 0.001$. ****, $p < 0.0001$.

(G) qPCR analysis of mRNA expression of SOX2 in a second derivation of 9 matched GSCs and DGCs. Student t-test was used to assess statistical significance with four technical replicates. ***, $p < 0.001$. ****, $p < 0.0001$.

(H) qPCR analysis of mRNA expression of OLIG2 in a second derivation of 9 matched GSCs and DGCs. Student t-test was used to assess statistical significance with four technical replicates. ***, $p < 0.001$. ****, $p < 0.0001$.

(I) qPCR analysis of mRNA expression of GFAP in a second derivation of 9 matched GSCs and DGCs. Student t-test was used to assess statistical significance with four technical replicates. ***, $p < 0.001$. ****, $p < 0.0001$.

(J) qPCR analysis of mRNA expression of ELOVL2, following treatment with 1.5uM of JQ1 for 48 hours in three GSCs (GSC387, GSC3565, and GSC23) with 6 technical replicates per condition. Student's t-test with Holm-Sidak multiple test corrections, (****, $p < 0.0001$)

(K) Same as (J) for KLHDC8A.

(L) Same as (J) for WSCD1.

(M) qPCR analysis of mRNA expression of MYC, following treatment with 1.5uM of JQ1 for 48 hours in three GSCs (GSC387, GSC3565, and GSC23). Student's t-test with Holm-Sidak multiple test corrections with six technical replicates (****, $p<0.0001$)

(N) Cell viability in the GSC3565 cell model was assessed over a 7-day time course following knockdown with two independent, non-overlapping shRNAs targeting ELOVL2 (shELOVL2.308, shELOVL2.843) or a non-targeting shRNA (shCONT). Two-way repeated measures ANOVA was used for statistical analysis with Dunnett's multiple hypothesis test correction with five technical replicates (****, $p<0.0001$). Inset shows qPCR analysis of mRNA expression of ELOVL2 in the GSC3565 tumor model following knockdown. One-way ANOVA was used for statistical analysis

with Dunnett's multiple hypothesis test correction with three technical replicates. ***, $p < 0.001$. ****, $p < 0.0001$.

(O) Cell viability in the GSC3565 cell model was assessed over a 7-day time course following knockdown with two independent, non-overlapping shRNAs targeting KLHDC8A (shKLHDC8A.1842, shKLHDC8A.883) or a non-targeting shRNA (shCONT). Two-way repeated measures ANOVA was used for statistical analysis with Dunnett's multiple hypothesis test correction with five technical replicates (****, $p<0.0001$). Inset shows qPCR analysis of mRNA expression of KLHDC8A in the GSC3565 tumor model following knockdown. One-way ANOVA was used for statistical analysis with Dunnett's multiple hypothesis test correction with three technical replicates. *, $p < 0.05$. ****, $p < 0.0001$.

(P) Cell viability in the GSC3565 cell model was assessed over a 7-day time course following knockdown with two independent, non-overlapping shRNAs targeting WSCD1 (shWSCD1.1087, shWSCD1.952) or a non-targeting shRNA (shCONT). Two-way repeated measures ANOVA was used for statistical analysis with Dunnett's multiple hypothesis test correction with five technical replicates (****, $p<0.0001$). qPCR analysis of mRNA expression of WSCD1 in the GSC3565 tumor model following knockdown. Two-way repeated measures ANOVA was used for statistical analysis with Dunnett's multiple hypothesis test correction with three technical replicates. ****, $p<0.0001$.

Figure S3

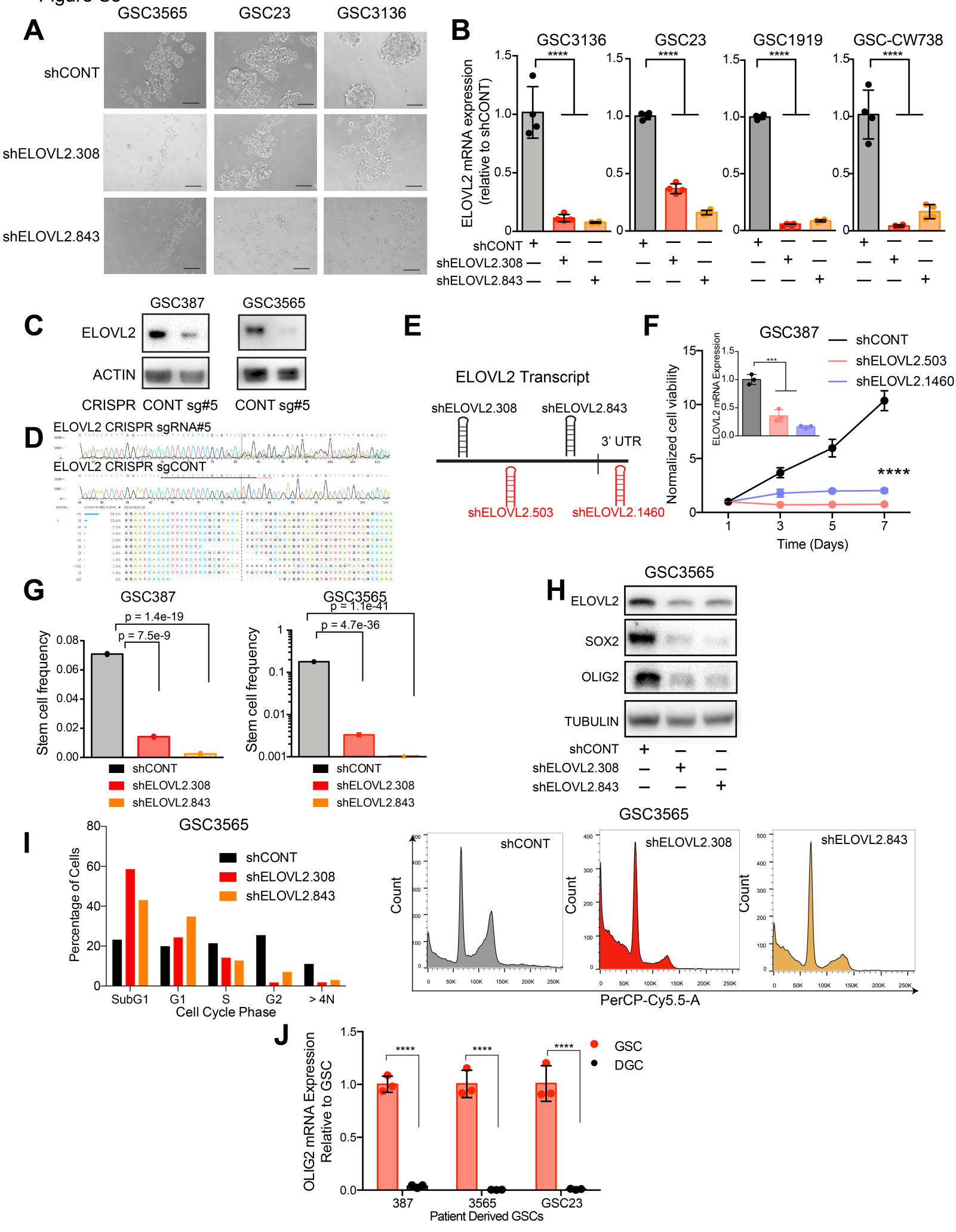
A
GSC3565
GSC23
GSC3136
shCONT
shELOVL2.308
shELOVL2.843
B
GSC3136
GSC23
GSC1919
GSC-CW738
ELOVL2 mRNA expression (relative to shCONT)
****
shCONT
shELOVL2.308
shELOVL2.843
C
GSC387
GSC3565
ELOVL2
ACTIN
CRISPR CONT sg#5
CONT sg#5
D
ELOVL2 CRISPR sgRNA#5
ELOVL2 CRISPR sgCONT
E
ELOVL2 Transcript
shELOVL2.308
shELOVL2.843
3' UTR
shELOVL2.503
shELOVL2.1460
F
GSC387
shCONT
shELOVL2.503
shELOVL2.1460
Normalized cell viability
ELOVL2 mRNA Expression
***
****
Time (Days)
G
GSC387
GSC3565
p = 1.4e-19
p = 7.5e-9
p = 1.1e-41
p = 4.7e-36
Stem cell frequency
shCONT
shELOVL2.308
shELOVL2.843
H
GSC3565
ELOVL2
SOX2
OLIG2
TUBULIN
shCONT
shELOVL2.308
shELOVL2.843
I
GSC3565
Percentage of Cells
SubG1
G1
S
G2
> 4N
Cell Cycle Phase
shCONT
shELOVL2.308
shELOVL2.843
Count
PerCP-Cy5.5-A
J
OLIG2 mRNA Expression Relative to GSC
****
GSC
DGC
387
3565
GSC23
Patient Derived GSCs

Figure S3. ELOVL2 knockdown and knockout impairs cell proliferation capacity in glioblastoma stem cells, related to Figure 4.

(A) Representative cell images 4 days following knockdown with two independent, non-overlapping shRNAs targeting ELOVL2 (shELOVL2.308, shELOVL2.843) or a non-targeting shRNA (shCONT). The scale bar represents 200 μm.

(B) qPCR analysis of mRNA expression of ELOVL2 in four GSCs following knockdown with two independent, non-overlapping shRNAs targeting ELOVL2 (shELOVL2.308, shELOVL2.843) or a non-targeting shRNA (shCONT). One-way ANOVA was used for statistical analysis with Dunnett's multiple hypothesis test correction with four technical replicates. ****, $p < 0.0001$.

(C) Western blot showing ELOVL2 protein levels following CRISPR-Cas9 mediated knockout of ELOVL2. Actin was used as a loading control.

(D) Genomic DNA flanking the ELOVL2 CRISPR-Cas9 cut site was PCR amplified and subjected to Sanger sequencing. Sequencing tracks from the non-targeting sgRNA (sgCONT) and sgRNA targeting ELOVL2 are displayed with insertion/deletion sites.

(E) Schematic of shRNAs targeting the ELOVL2 mRNA.

(F) Cell viability in GSC387 over a 7-day time course following knockdown with two independent, non-overlapping shRNAs targeting ELOVL2 (shELOVL2.503, shELOVL2.1460) or a non-targeting shRNA (shCONT). 5 technical replicates were used for each condition. Two-way repeated measures ANOVA with Dunnett's multiple hypothesis test correction (****, $p < 0.0001$). Inset shows qPCR demonstrating ELOVL2 expression following treatment with two independent non-overlapping shRNAs targeting ELOVL2 (***, $p < 0.001$).

(G) Quantification of stem cell frequency from in vitro limiting dilution assay.

(H) Western blot following ELOVL2 knockdown with two independent, non-overlapping shRNAs targeting ELOVL2 (shELOVL2.308, shELOVL2.843) or a non-targeting shRNA (shCONT). Tubulin was used as a loading control.

(I) Cell cycle analysis of the GSC3565 cell model 3 days following knockdown with two independent, non-overlapping shRNAs targeting ELOVL2 (shELOVL2.308, shELOVL2.843) or a non-targeting shRNA (shCONT).

(J) qPCR analysis of OLIG2 mRNA expression in paired GSCs and DGCs derived from GSC387, GSC3565, and GSC23. Two-way ANOVA with Sidak multiple test correction was used for statistical analysis. ****, $p < 0.0001$.

Figure S4

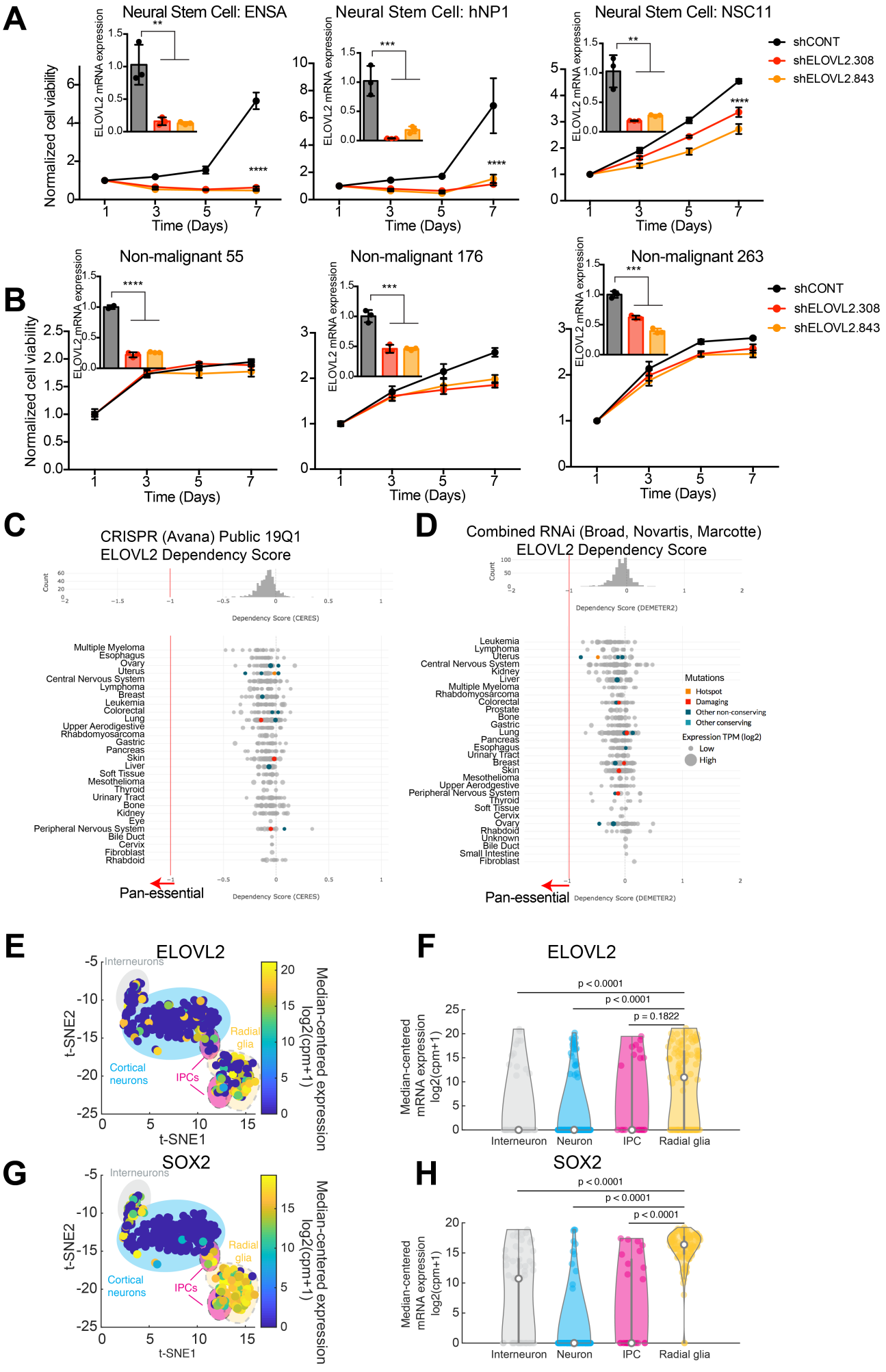
A
Neural Stem Cell: ENSA
Neural Stem Cell: hNP1
Neural Stem Cell: NSC11
ELOVL2 mRNA expression
Normalized cell viability
Time (Days)
shCONT
shELOVL2.308
shELOVL2.843
B
Non-malignant 55
Non-malignant 176
Non-malignant 263
C
CRISPR (Avana) Public 19Q1
ELOVL2 Dependency Score
Dependency Score (CERES)
Pan-essential
D
Combined RNAi (Broad, Novartis, Marcotte)
ELOVL2 Dependency Score
Dependency Score (DEMETER2)
Mutations
Hotspot
Damaging
Other non-conserving
Other conserving
Expression TPM (log2)
Low
High
E
ELOVL2
Interneurons
Radial glia
Cortical neurons
IPCs
t-SNE1
t-SNE2
Median-centered expression log2(cpm+1)
F
ELOVL2
p < 0.0001
p < 0.0001
p = 0.1822
Median-centered mRNA expression log2(cpm+1)
Interneuron
Neuron
IPC
Radial glia
G
SOX2
H
SOX2
p < 0.0001
p < 0.0001
p < 0.0001

Figure S4. ELOVL2 marks stem cell populations and is not a pan-essential gene, related to Figure 4.

(A) Cell viability in three neural stem cells (ENSA, hNP1, and NSC11) was assessed over a 7-day time course following knockdown with two independent, non-overlapping shRNAs targeting ELOVL2 (shELOVL2.308, shELOVL2.843) or a non-targeting shRNA (shCONT). Two-way repeated measures ANOVA was used for statistical analysis with Dunnett's multiple hypothesis test correction with five technical replicates (****, $p<0.0001$). Inset shows qPCR analysis of mRNA expression of ELOVL2 following knockdown. One-way ANOVA was used for statistical analysis with Dunnett's multiple hypothesis test correction with three technical replicates. **, $p < 0.01$. ***, $p < 0.001$.

(B) Cell viability in three non-malignant neural cells derived from epilepsy tissue resection specimens (NM55, NM176, and NM263) was assessed over a 7-day time course following knockdown with two independent, non-overlapping shRNAs targeting ELOVL2 (shELOVL2.308, shELOVL2.843) or a non-targeting shRNA (shCONT). Inset shows qPCR analysis of mRNA expression of ELOVL2 following knockdown. One-way ANOVA was used for statistical analysis with Dunnett's multiple hypothesis test correction with three technical replicates. ***, $p < 0.001$. ****, $p < 0.0001$.

(C) ELOVL2 dependency score in a whole genome CRISPR-Cas9 screen across 558 cancer cell lines. A lower score means that a gene is more likely to be dependent in a given cell line. A score of 0 is equivalent to a gene that is not essential whereas a score of -1 corresponds to the median of all common essential genes. Data were derived from the Cancer Dependency Map (www.depmap.org). Dependency score is calculated using the CERES algorithm.

(D) ELOVL2 dependency score in a whole genome shRNA screen across 711 cancer cell lines. Dependency score is calculated using the DEMETER2 algorithm.

(E) Single-cell RNA-sequencing (scRNA-seq) data from normal brain specimens derived from (31) presented as a t-Distributed Stochastic Neighbor Embedding (t-SNE) plot demonstrating expression of ELOVL2 across brain cell types. Data is presented as median centered mRNA expression in counts per million (CPM). IPC denotes intermediate progenitor cells.

(F) Quantification of data in (E).

(G) Same as (E) for SOX2 mRNA expression.

(H) Quantification of data in (G).

Figure S5

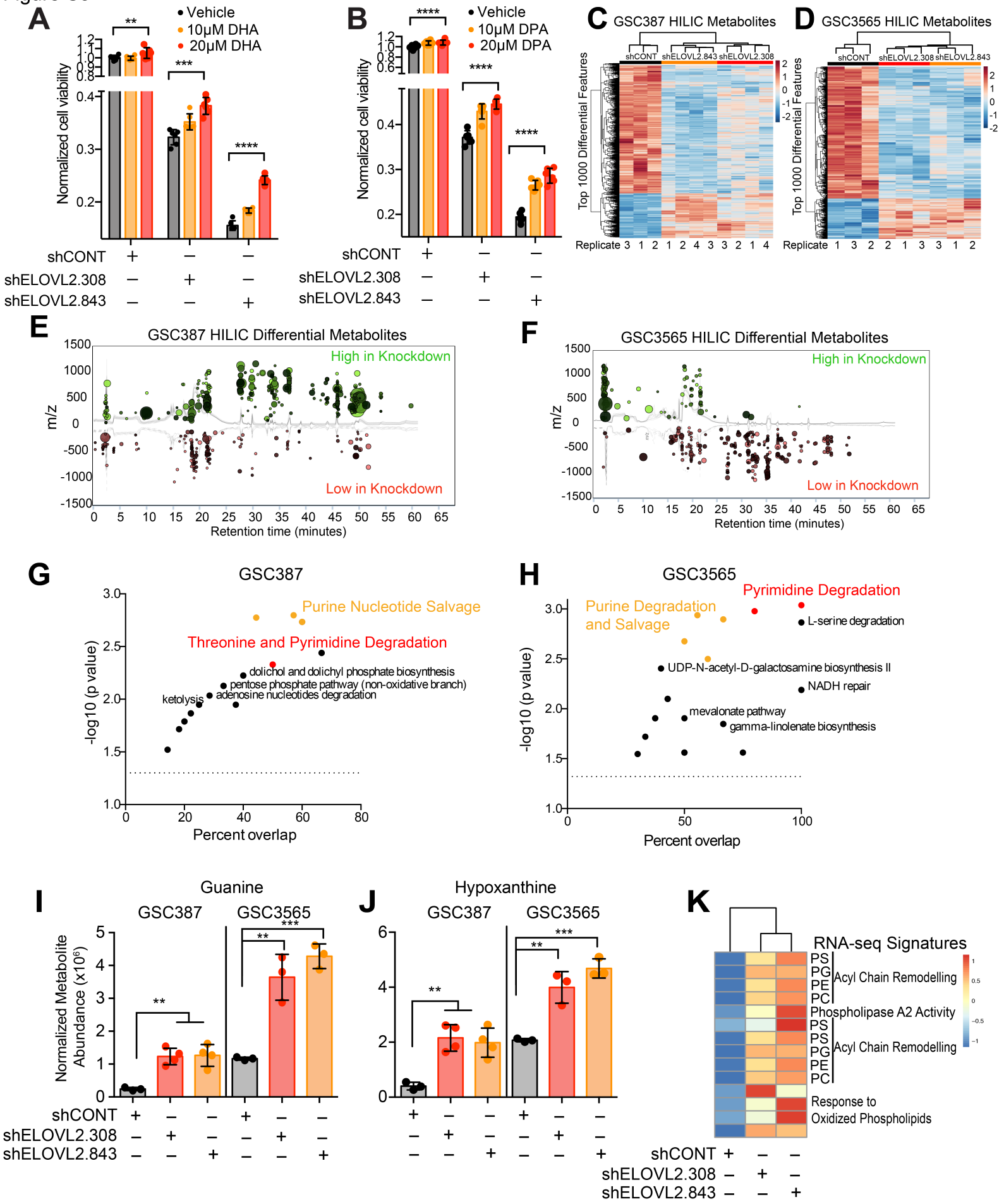
A
Vehicle
10μM DHA
20μM DHA
Normalized cell viability
shCONT
shELOVL2.308
shELOVL2.843
B
Vehicle
10μM DPA
20μM DPA
Normalized cell viability
shCONT
shELOVL2.308
shELOVL2.843
C GSC387 HILIC Metabolites
shCONT shELOVL2.843 shELOVL2.308
Top 1000 Differential Features
Replicate 3 1 2 1 2 4 3 3 2 1 4
D GSC3565 HILIC Metabolites
shCONT shELOVL2.308 shELOVL2.843
Top 1000 Differential Features
Replicate 1 3 2 2 1 3 3 1 2
E
GSC387 HILIC Differential Metabolites
High in Knockdown
Low in Knockdown
m/z
Retention time (minutes)
F
GSC3565 HILIC Differential Metabolites
High in Knockdown
Low in Knockdown
m/z
Retention time (minutes)
G
GSC387
Purine Nucleotide Salvage
Threonine and Pyrimidine Degradation
dolichol and dolichyl phosphate biosynthesis
pentose phosphate pathway (non-oxidative branch)
ketolysis
adenosine nucleotides degradation
-log10 (p value)
Percent overlap
H
GSC3565
Pyrimidine Degradation
Purine Degradation and Salvage
L-serine degradation
UDP-N-acetyl-D-galactosamine biosynthesis II
NADH repair
mevalonate pathway
gamma-linolenate biosynthesis
-log10 (p value)
Percent overlap
I
Guanine
GSC387
GSC3565
Normalized Metabolite Abundance (x10⁶)
shCONT
shELOVL2.308
shELOVL2.843
J
Hypoxanthine
GSC387
GSC3565
K
RNA-seq Signatures
PS
PG
PE
PC
Acyl Chain Remodelling
Phospholipase A2 Activity
PS
PS
PG
PE
PC
Acyl Chain Remodelling
Response to Oxidized Phospholipids
shCONT
shELOVL2.308
shELOVL2.843

Figure S5. Global metabolomics analysis reveals enrichment in purine salvage and pyrimidine degradation pathways following ELOVL2 knockdown, related to Figure 5.

(A) Cell viability in GSC387 following knockdown with two independent, non-overlapping shRNAs targeting ELOVL2 or a non-targeting shRNA (shCONT). Cells were treated with vehicle, 10 μM, or 20 μM of docosahexaenoic acid (DHA). Statistical significance was assessed using two-way ANOVA with Dunnett multiple test correction with six technical replicates. **; $p < 0.01$; ***, $p < 0.001$; ****, $p < 0.0001$.

(B) Same as (A) with docosapentaenoic acid (DPA).

(C) Heatmap displaying the top 1,000 differential mass spectrometry features in the negative mode (HILIC) in the GSC387 model following knockdown with two independent, non-overlapping shRNAs targeting ELOVL2 (shELOVL2.308, shELOVL2.843) or a non-targeting shRNA (shCONT).

(D) Heatmap displaying the top 1,000 differential mass spectrometry features in the negative mode (HILIC) in the GSC3565 model following knockdown with two independent, non-overlapping shRNAs targeting ELOVL2 (shELOVL2.308, shELOVL2.843) or a non-targeting shRNA (shCONT).

(E) Pathway cloud plot showing differential mass spectrometry features in the GSC387 model when analyzed in the negative mode (HILIC).

(F) Pathway cloud plot showing differential mass spectrometry features in the GSC3565 model when analyzed in the negative mode (HILIC).

(G) Pathway analysis of differential putative metabolites in the GSC387 model following ELOVL2 knockdown as determined through mass spectrometry in the negative mode (HILIC).

(H) Pathway analysis of differential putative metabolites in the GSC387 model following ELOVL2 knockdown as determined through mass spectrometry in the negative mode (HILIC).

(I) Metabolite abundance of guanine following knockdown with two independent, non-overlapping shRNAs targeting ELOVL2 (shELOVL2.308, shELOVL2.843) or a non-targeting shRNA (shCONT). One-way ordinary ANOVA was used for comparisons with three technical replicates. **, $p < 0.01$. ***, $p < 0.001$.

(J) Metabolite abundance of hypoxanthine following knockdown with two independent, non-overlapping shRNAs targeting ELOVL2 (shELOVL2.308, shELOVL2.843) or a non-targeting shRNA (shCONT). One-way ordinary ANOVA was used for comparisons with three technical replicates. **, $p < 0.01$. ***, $p < 0.001$.

(K) Heatmap displays differential transcriptional signatures derived from RNA-sequencing following knockdown with two independent, non-overlapping shRNAs targeting ELOVL2 or a non-targeting shRNA (shCONT).

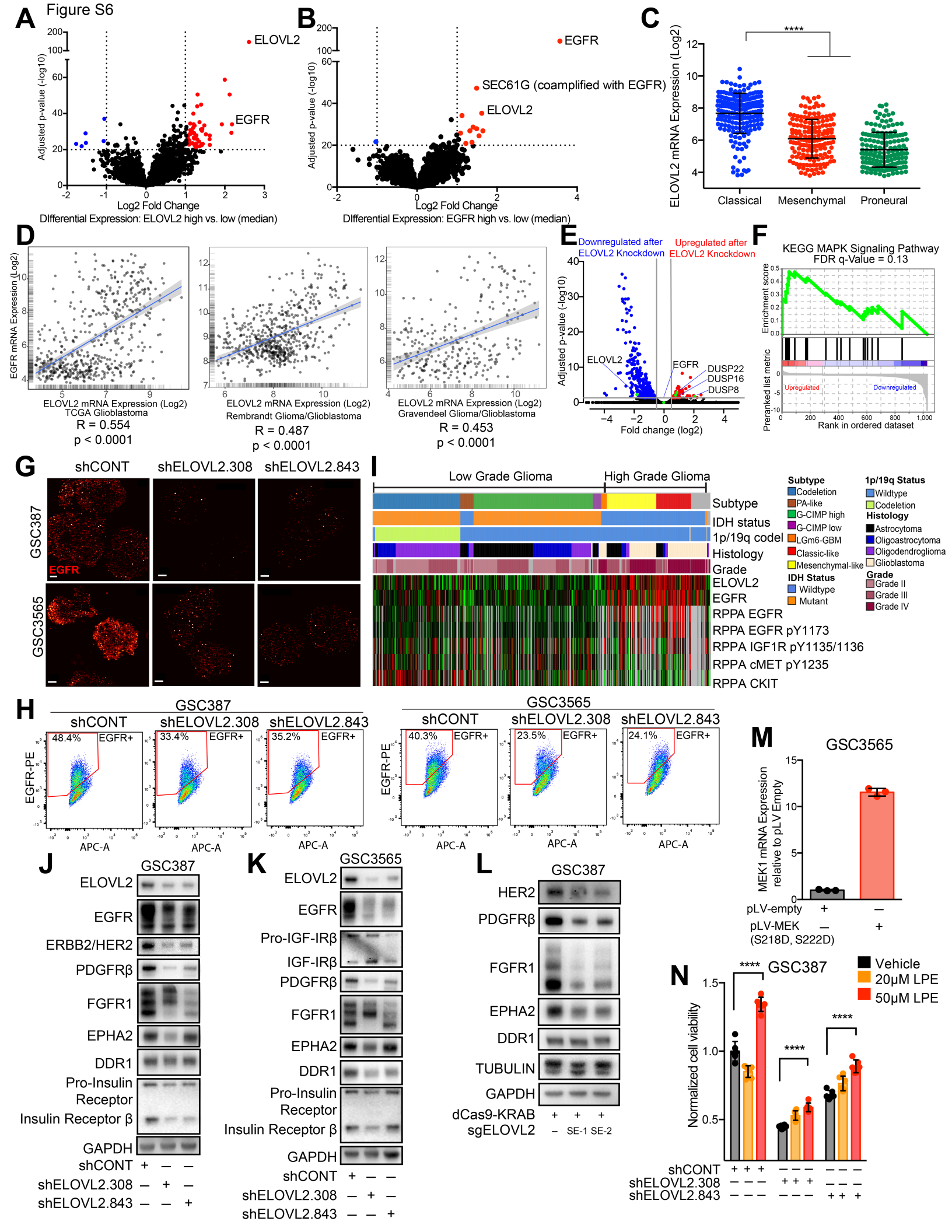
Figure S6
A
ELOVL2
EGFR
Adjusted p-value (-log10)
Log2 Fold Change
DIfferential Expression: ELOVL2 high vs. low (median)
B
EGFR
SEC61G (coamplified with EGFR)
ELOVL2
Adjusted p-value (-log10)
Log2 Fold Change
DIfferential Expression: EGFR high vs. low (median)
C
****
ELOVL2 mRNA Expression (Log2)
Classical
Mesenchymal
Proneural
D
EGFR mRNA Expression (Log2)
ELOVL2 mRNA Expression (Log2)
TCGA Glioblastoma
R = 0.554
p < 0.0001
ELOVL2 mRNA Expression (Log2)
Rembrandt Glioma/Glioblastoma
R = 0.487
p < 0.0001
ELOVL2 mRNA Expression (Log2)
Gravendeel Glioma/Glioblastoma
R = 0.453
p < 0.0001
E
Downregulated after ELOVL2 Knockdown
Upregulated after ELOVL2 Knockdown
Adjusted p-value (-log10)
ELOVL2
EGFR
DUSP22
DUSP16
DUSP8
Fold change (log2)
F
KEGG MAPK Signaling Pathway
FDR q-Value = 0.13
Enrichment score
Upregulated
Downregulated
Preranked list metric
Rank in ordered dataset
G
shCONT
shELOVL2.308
shELOVL2.843
GSC387
GSC3565
EGFR
I
Low Grade Glioma
High Grade Glioma
Subtype
IDH status
1p/19q codel
Histology
Grade
ELOVL2
EGFR
RPPA EGFR
RPPA EGFR pY1173
RPPA IGF1R pY1135/1136
RPPA cMET pY1235
RPPA CKIT
Subtype
Codeletion
PA-like
G-CIMP high
G-CIMP low
LGm6-GBM
Classic-like
Mesenchymal-like
IDH Status
Wildtype
Mutant
1p/19q Status
Wildtype
Codeletion
Histology
Astrocytoma
Oligoastrocytoma
Oligodendroglioma
Glioblastoma
Grade
Grade II
Grade III
Grade IV
H
GSC387
shCONT
shELOVL2.308
shELOVL2.843
48.4% EGFR+
33.4% EGFR+
35.2% EGFR+
GSC3565
40.3% EGFR+
23.5% EGFR+
24.1% EGFR+
EGFR-PE
APC-A
M
GSC3565
MEK1 mRNA Expression relative to pLV Empty
pLV-empty
pLV-MEK (S218D, S222D)
J
GSC387
ELOVL2
EGFR
ERBB2/HER2
PDGFRβ
FGFR1
EPHA2
DDR1
Pro-Insulin Receptor
Insulin Receptor β
GAPDH
shCONT
shELOVL2.308
shELOVL2.843
K
GSC3565
ELOVL2
EGFR
Pro-IGF-IRβ
IGF-IRβ
PDGFRβ
FGFR1
EPHA2
DDR1
Pro-Insulin Receptor
Insulin Receptor β
GAPDH
shCONT
shELOVL2.308
shELOVL2.843
L
GSC387
HER2
PDGFRβ
FGFR1
EPHA2
DDR1
TUBULIN
GAPDH
dCas9-KRAB
sgELOVL2
SE-1
SE-2
N
GSC387
Vehicle
20μM LPE
50μM LPE
Normalized cell viability
shCONT
shELOVL2.308
shELOVL2.843

Figure S6. Polyunsaturated fatty acid synthesis supports EGFR signaling in glioblastoma stem cells, related to Figure 6.

(A) Volcano plot demonstrating differentially expressed genes in the TCGA HG-U133A microarray glioblastoma dataset between ELOVL2 high and ELOVL2 low specimens, using the median ELOVL2 mRNA expression as a cutoff.

(B) Volcano plot demonstrating differentially expressed genes in the TCGA HG-U133A microarray glioblastoma dataset between EGFR high and EGFR low specimens, using the median EGFR mRNA expression as a cutoff.

(C) ELOVL2 mRNA expression from The Cancer Genome Atlas (TCGA) HG-U133A glioblastoma microarray between three transcriptional subtypes. Statistical significance was assessed using ordinary one-way ANOVA with Tukey multiple comparison correction. ****, $p < 0.0001$ for all pairwise comparisons.

(D) Correlation between ELOVL2 and EGFR was calculated in (left) the TCGA HG-U133A glioblastoma dataset, (middle) the Rembrandt glioma/glioblastoma dataset, and (right) the Gravendeel glioma/glioblastoma dataset.

(E) Volcano plot showing results of differential expression RNA-seq analysis in GSC387 and GSC3565.

(F) Gene set enrichment plot for the KEGG MAPK Signaling pathway. Genes were ranked based on the p-value significance of their differential expression between shCONT and shELOVL2.308/ shELOVL2.843. FDR-corrected q-value = 0.13.

(G) Super-resolution stochastic optical reconstruction microscopy (STORM) imaging of EGFR following knockdown with two independent, non-overlapping shRNAs targeting ELOVL2 (shELOVL2.308, shELOVL2.843) or a non-targeting shRNA (shCONT) in the GSC387 and GSC3565 model. Scalebar shows 2 μm.

(H) Flow cytometry analysis of cell surface EGFR following knockdown with two independent, non-overlapping shRNAs targeting ELOVL2 or a non-targeting shRNA (shCONT) in GSC387 and GSC3565 with three technical replicates.

(I) Heatmap showing glioma subtype and clinical characteristics from the TCGA dataset. ELOVL2 and EGFR mRNA expression from the HG-U133A glioma microarray is presented with reverse phase protein array (RPPA) data for receptor tyrosine kinases.

(J) Western blot in GSC387 following knockdown with two independent, non-overlapping shRNAs targeting ELOVL2 (shELOVL2.308, shELOVL2.843) or a non-targeting shRNA (shCONT). GAPDH is used as a loading control.

(K) Western blot in GSC3565 following knockdown with two independent, non-overlapping shRNAs targeting ELOVL2 (shELOVL2.308, shELOVL2.843) or a non-targeting shRNA (shCONT). GAPDH is used as a loading control.

(L) Western blot GSC387 cells following treatment with dCas9-KRAB and two sgRNAs targeting the ELOVL2 super-enhancer critical region or an empty dCas9-KRAB vector. TUBULIN and GAPDH are used as loading controls.

(M) qPCR analysis of mRNA expression of MEK1 (MAP2K1) in GSC3565 following treatment with a constitutive active MEK (S218D, S222D) or an empty vector.

(N) Cell viability in GSC387 following knockdown with two independent, non-overlapping shRNAs targeting ELOVL2 or a non-targeting shRNA (shCONT). Cells were treated with vehicle, 20 μM, or

50 μM of lysophosphatidylethanolamine. Statistical significance was assessed using two-way ANOVA with Dunnett multiple test correction with six technical replicates. ****, $p < 0.0001$.

Figure S7

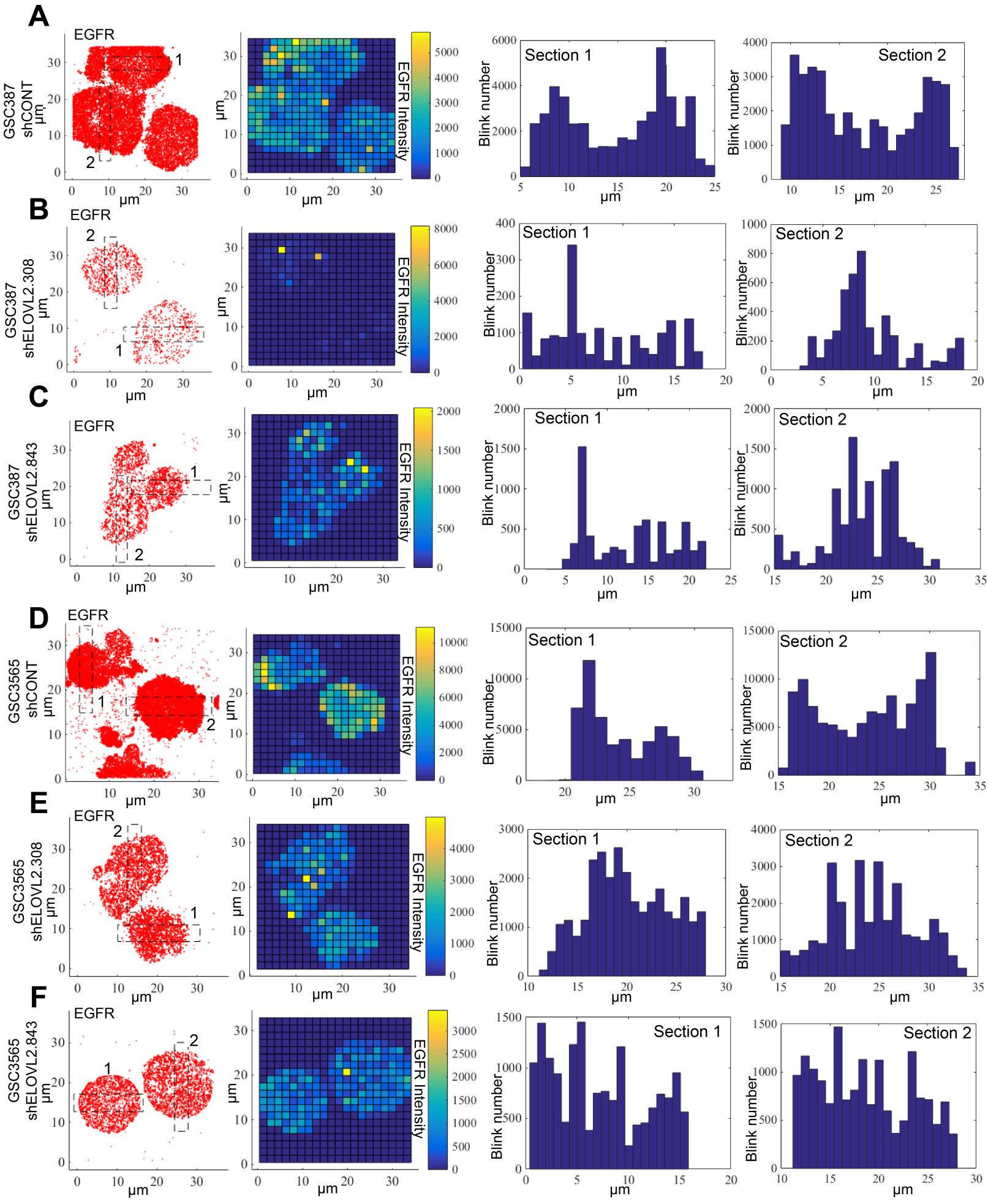
A
EGFR
GSC387
shCONT
B
GSC387
shELOVL2.308
C
GSC387
shELOVL2.843
D
GSC3565
shCONT
E
GSC3565
shELOVL2.308
F
GSC3565
shELOVL2.843
μm
EGFR Intensity
Blink number
Section 1
Section 2

Figure S7. ELOVL2 knockdown abolishes preferential localization of EGFR to cell membrane, related to Figure 6.

(A) Stochastic optical reconstruction microscopy (STORM) imaging of GSC387 following treatment with a non-targeting shRNA (shCONT) showing (Left) EGFR density with bivariate histogram plot of blink number (right) histogram of blink numbers corresponding to EGFR density across two different 4 μm sections that cross the center of the cell.

(B) Same as (A) following treatment with an shRNA targeting ELOVL2 (shELOVL2.308).

(C) Same as (A) following treatment with an shRNA targeting ELOVL2 (shELOVL2.843).

(D) Stochastic optical reconstruction microscopy (STORM) imaging of GSC3565 following treatment with a non-targeting shRNA (shCONT) showing (Left) EGFR density with bivariate histogram plot of blink number (right) histogram of blink numbers corresponding to EGFR density across two different 4 μm sections that cross the center of the cell.

(E) Same as (D) following treatment with an shRNA targeting ELOVL2 (shELOVL2.308).

(F) Same as (D) following treatment with an shRNA targeting ELOVL2 (shELOVL2.843).

Figure S8

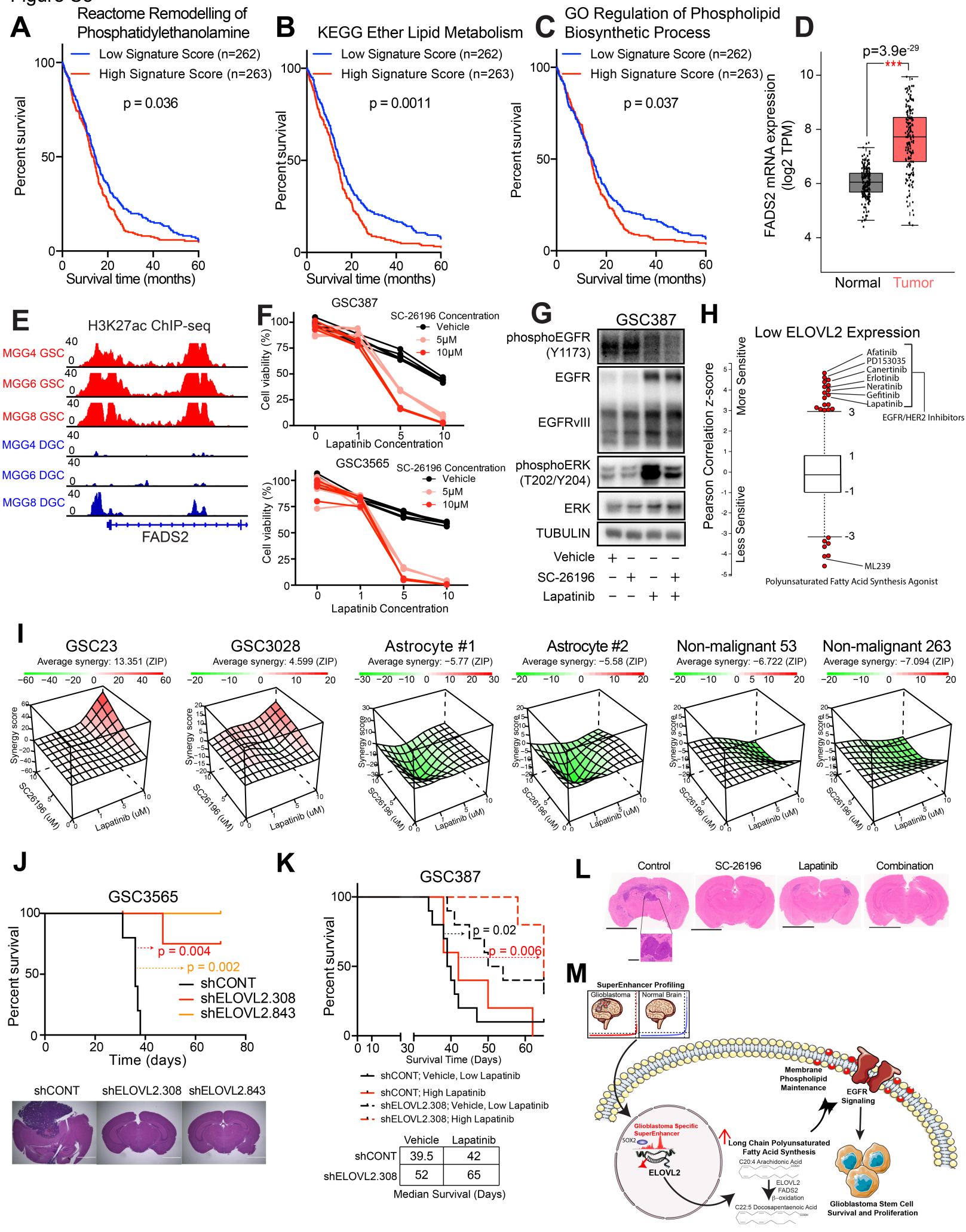
A
Reactome Remodelling of Phosphatidylethanolamine
Low Signature Score (n=262)
High Signature Score (n=263)
p = 0.036
Percent survival
Survival time (months)
B
KEGG Ether Lipid Metabolism
Low Signature Score (n=262)
High Signature Score (n=263)
p = 0.0011
Percent survival
Survival time (months)
C
GO Regulation of Phospholipid Biosynthetic Process
Low Signature Score (n=262)
High Signature Score (n=263)
p = 0.037
Percent survival
Survival time (months)
D
p=3.9e-29
***
FADS2 mRNA expression (log2 TPM)
Normal
Tumor
E
H3K27ac ChIP-seq
MGG4 GSC
MGG6 GSC
MGG8 GSC
MGG4 DGC
MGG6 DGC
MGG8 DGC
FADS2
F
GSC387
SC-26196 Concentration
Vehicle
5μM
10μM
Cell viability (%)
Lapatinib Concentration
GSC3565
SC-26196 Concentration
Vehicle
5μM
10μM
Cell viability (%)
Lapatinib Concentration
G
GSC387
phosphoEGFR (Y1173)
EGFR
EGFRvIII
phosphoERK (T202/Y204)
ERK
TUBULIN
Vehicle + − − −
SC-26196 − + − +
Lapatinib − − + +
H
Low ELOVL2 Expression
Pearson Correlation z-score
More Sensitive
Less Sensitive
Afatinib
PD153035
Canertinib
Erlotinib
Neratinib
Gefitinib
Lapatinib
EGFR/HER2 Inhibitors
ML239
Polyunsaturated Fatty Acid Synthesis Agonist
I
GSC23
Average synergy: 13.351 (ZIP)
GSC3028
Average synergy: 4.599 (ZIP)
Astrocyte #1
Average synergy: −5.77 (ZIP)
Astrocyte #2
Average synergy: −5.58 (ZIP)
Non-malignant 53
Average synergy: −6.722 (ZIP)
Non-malignant 263
Average synergy: −7.094 (ZIP)
Synergy score
SC26196 (uM)
Lapatinib (uM)
J
GSC3565
p = 0.004
p = 0.002
shCONT
shELOVL2.308
shELOVL2.843
Percent survival
Time (days)
shCONT
shELOVL2.308
shELOVL2.843
K
GSC387
p = 0.02
p = 0.006
Percent survival
Survival Time (Days)
shCONT; Vehicle, Low Lapatinib
shCONT; High Lapatinib
shELOVL2.308; Vehicle, Low Lapatinib
shELOVL2.308; High Lapatinib
Vehicle Lapatinib
shCONT 39.5 42
shELOVL2.308 52 65
Median Survival (Days)
L
Control
SC-26196
Lapatinib
Combination
M
SuperEnhancer Profiling
Glioblastoma
Normal Brain
Membrane Phospholipid Maintenance
EGFR Signaling
Glioblastoma Specific SuperEnhancer
SOX2
ELOVL2
Long Chain Polyunsaturated Fatty Acid Synthesis
C20:4 Arachidonic Acid
ELOVL2
FADS2
β-oxidation
C22:5 Docosapentaenoic Acid
Glioblastoma Stem Cell Survival and Proliferation

Figure S8. Polyunsaturated fatty acid synthesis is a potential clinical target in glioblastoma, related to Figure 7.

(A) Kaplan-Meier curve showing survival of patients in the TCGA HG-U133A glioblastoma dataset stratified based on signature score from the "Reactome remodeling of phosphatidylethanolamine" signature. Log-rank analysis (p=0.0036, "Signature low" n=262, "Signature high" n=263).

(B) Kaplan-Meier curve showing survival of patients in the TCGA HG-U133A glioblastoma dataset stratified based on signature score from the "KEGG ether lipid metabolism" signature. Log-rank analysis (p=0.0011, "Signature low" n=262, "Signature high" n=263).

(C) Kaplan-Meier curve showing survival of patients in the TCGA HG-U133A glioblastoma dataset stratified based on signature score from the "GO regulation of phospholipid biosynthetic process" signature. Log-rank analysis (p=0.037, "Signature low" n=262, "Signature high" n=263).

(D) mRNA expression TPM values in normal brain (GTEx, n=207) and glioblastoma (TCGA, n=163) from RNA-seq data for FADS2. Four-way ANOVA controlling for sex, age, and ethnicity with Benjamini and Hochberg false discovery rate (FDR) method, p= 3.9e-29.

(E) H3K27ac signal at the FADS2 promoter region in three matched GSCs and DGCs (MGG4, MGG6, and MGG8). Data was derived from (26).

(F) Cell viability of GSC387 and GSC3565 following combinatorial treatment with lapatinib or SC-26196. Six technical replicates were used.

(G) Western blot following treatment with lapatinib (5 μM), SC-26196 (10 μM), or a combination. Tubulin was used as a loading control.

(H) Cancer cell viability data from 860 cell lines in response to 481 compounds is stratified based on ELOVL2 expression. For each compound, the Pearson correlation z-score between drug sensitivity and ELOVL2 expression is plotted with positive values indicating that low ELOVL2 expression is associated with increased sensitivity to the compound and positive values indicating that low ELOVL2 expression is associated with decreased sensitivity to the compound. Data was accessed from the Cancer Therapeutics Response Portal (https://portals.broadinstitute.org/ctrp.v2.1/). Cells in any growth mode and primary site/subtype were considered for analysis.

(I) In vitro synergy diagram of combinatorial lapatinib and SC-26196 treatment. ZIP score was used to assess synergy (55).

(J) (Top) Kaplan-Meier curve showing survival of mice following implantation with GSC3565 following knockdown with two independent, non-overlapping shRNAs targeting ELOVL2 or a non-targeting shRNA (shCONT). n=5 mice per arm. shCONT vs. shELOVL2.308, p = 0.004. shCONT vs. shELOVL2.843, p = 0.002. (Bottom) Hematoxylin and eosin staining of brains following implantation with GSC387 following shCONT or shELOVL2 treatment.

(K) Kaplan-Meier curve showing survival of mice following implantation with GSC387 following treatment with an shRNA targeting ELOVL2 (shELOVL2.308) or a non-targeting control (shCONT). Mice were treated by oral gavage with vehicle control, low dose lapatinib (20 mg/kg), or high dose lapatinib (40 mg/kg). Vehicle/low dose lapatinib group (n=10). High dose lapatinib group (n=5).

(L) Hematoxylin and eosin staining of brains following implantation with GSC387 and treatment as shown in Figure 7K. Scale bar indicates 3mm in upper panels, and 400μM in the callout.

(M) Model diagram for the mechanisms underlying ELOVL2 activation and function in glioblastoma

stem cells. In glioblastoma stem cells, a cell-state specific super-enhancer supported by SOX2 drives ELOVL2 expression. ELOVL2 functions to increase long chain polyunsaturated fatty acid synthesis, which supports cell membrane architecture and efficient EGFR signaling.